



## Continuous determination of hydrogen peroxide formed in advanced oxidation and electrochemical processes

Tae-Mun Hwang<sup>a,\*</sup>, Byung Soo Oh<sup>b</sup>, Yeojoon Yoon<sup>c</sup>, Minhwan Kwon<sup>c</sup>, Joonwun Kang<sup>c</sup>

<sup>a</sup>Water Resources and Environmental Research Division, Korea Institute of Construction Technology 2311, Deawha-dong, Ilsan-Gu, Goyang-Si, Gyeonggi-Do 411-712, Korea

Tel. +82 31 910 0765; Fax: +82 31 910 0291; email: taemun@kict.re.kr

<sup>b</sup>LG Electronics Inc. 16 Woomyeon-dong, Seocho-gu, Seoul 137-724, South Korea

<sup>c</sup>Department of Environmental Engineering, Yonsei University, 234 Maeji, Heungup, Wonju 220-710, Korea

Received 25 December 2011; Accepted 10 February 2012

### ABSTRACT

A hydrogen peroxide (H<sub>2</sub>O<sub>2</sub>) auto-analyzer was developed to continuously detect H<sub>2</sub>O<sub>2</sub> present in water, using a flow injection analysis (FIA) technique, during several advanced oxidation processes (AOPs) involving H<sub>2</sub>O<sub>2</sub>, such as ozone/H<sub>2</sub>O<sub>2</sub>, UV/H<sub>2</sub>O<sub>2</sub>, and ozone/UV, and an electrochemical process. The analytical method was based on a fluorometric method, using the reaction of *p*-hydroxyphenyl acetic acid and H<sub>2</sub>O<sub>2</sub> in the presence of peroxidase enzyme. H<sub>2</sub>O<sub>2</sub> was analyzed within the high (100–2,000 µg/L) and low (0–500 µg/L) concentration ranges, using both long and short reaction coils, respectively. The standard deviation and detection limit were 0.5 and 1.6 µg/L, respectively, and the coefficient of variation at 1 µg/L was 7.8%. This study also investigated the effects of Na<sub>2</sub>S<sub>2</sub>O<sub>3</sub> and NH<sub>4</sub>Cl, which were used to quench the ozone and hypochlorous acid (HOCl) present in the samples, on the measurement of H<sub>2</sub>O<sub>2</sub> during the ozone-based AOPs and electrochemical process.

**Keywords:** Hydrogen peroxide auto-analyzer; Flow injection analysis; Advanced oxidation process

### 1. Introduction

Hydrogen peroxide (H<sub>2</sub>O<sub>2</sub>) is widely used as an initiator in advanced oxidation processes (AOPs), where it can increase the rate of hydroxyl radical (.OH) formation due to the reaction between ozone and its conjugate base, HO<sub>2</sub><sup>-</sup> [1]. Therefore, the utility of AOPs involving H<sub>2</sub>O<sub>2</sub> has recently increased for the effective oxidation of hazardous pollutants in water [2]. Especially, in the ozone/H<sub>2</sub>O<sub>2</sub>, UV/H<sub>2</sub>O<sub>2</sub>, and ozone/UV AOPs, since their ability to oxidize greatly depends on the H<sub>2</sub>O<sub>2</sub> experimental conditions, in terms of injection dosage and residual concentrations,

the precise and simple measurement of H<sub>2</sub>O<sub>2</sub> is significantly important for engineers to deal with these processes under the optimum operation conditions [1]. In this study, the UV/H<sub>2</sub>O<sub>2</sub>, and ozone/UV processes were selected as target processes for observing the residual H<sub>2</sub>O<sub>2</sub>. The direct degradation of H<sub>2</sub>O<sub>2</sub> in the UV/H<sub>2</sub>O<sub>2</sub> process and the formation pattern in ozone/UV process were able to be observed. Meanwhile, the utility of the electrochemical process in the field of water treatment, for the purposes of oxidation and disinfection, has only recently been realized. The electrochemical process, in general, produces mixed oxidants, such as hypochlorous acid (HOCl), ozone, H<sub>2</sub>O<sub>2</sub>, and several radicals (e.g. .OH, .O, .O<sub>2</sub><sup>-</sup>) [3]. However, there has been no success in the separation

\*Corresponding author.

and determination of these mixed oxidants and, thus, this study made great efforts to measure the  $\text{H}_2\text{O}_2$  formed during the electrolysis of water.

Various techniques for the analysis of  $\text{H}_2\text{O}_2$  have been reported over the years; early studies on  $\text{H}_2\text{O}_2$  in precipitation were performed using iodometric techniques, and then the luminol chemiluminescence method provided the first approach for determining  $\text{H}_2\text{O}_2$  at the 10 nM level [4]. Thereafter, the luminol technique has been modified with the use of hemin as a catalyst [5]. In 1985, for the determination of  $\text{H}_2\text{O}_2$  in the liquid phase, an automated analytical technique was developed using a fluorometric method with peroxidase, an enzyme characterized by its selectivity toward hydroperoxides [6]. In the presence of *p*-hydroxyphenyl acetic acid, the enzyme peroxidase catalyzes the reduction of  $\text{H}_2\text{O}_2$ , via the following reaction [7]:



The dimeric product fluoresces with peak excitation and emission wavelengths of 320 and 400 nm,

respectively [7]. The stoichiometry of reaction (1) indicates that one dimer is formed for every hydroperoxide ( $-\text{O}-\text{O}-\text{H}$ ) bond broken. The fluorescence of this dimer is, therefore, directly proportional to the peroxide concentration. In this study, since the peroxidase fluorometric method, compared to other methods, is hardly affected by interferences commonly found in environmental aqueous samples, an instrument (an  $\text{H}_2\text{O}_2$  auto-analyzer) was developed using an automated analytical technique based on this fluorometric method, which made the continuous measurement of the  $\text{H}_2\text{O}_2$  present in water samples possible using flow injection analysis (FIA). For its practical application, the  $\text{H}_2\text{O}_2$  auto-analyzer was tested in order to measure the residual  $\text{H}_2\text{O}_2$  concentrations during several processes, such as the UV/ $\text{H}_2\text{O}_2$ , ozone/UV, and electrochemical processes.

## 2. Experimental

### 2.1. Development of $\text{H}_2\text{O}_2$ auto-analyzer

Fig. 1 shows the schematic diagram of the FIA  $\text{H}_2\text{O}_2$  auto-analyzer developed in this study. Three DC drive pumps (Cole-Parmer Peristaltic pump, USA)

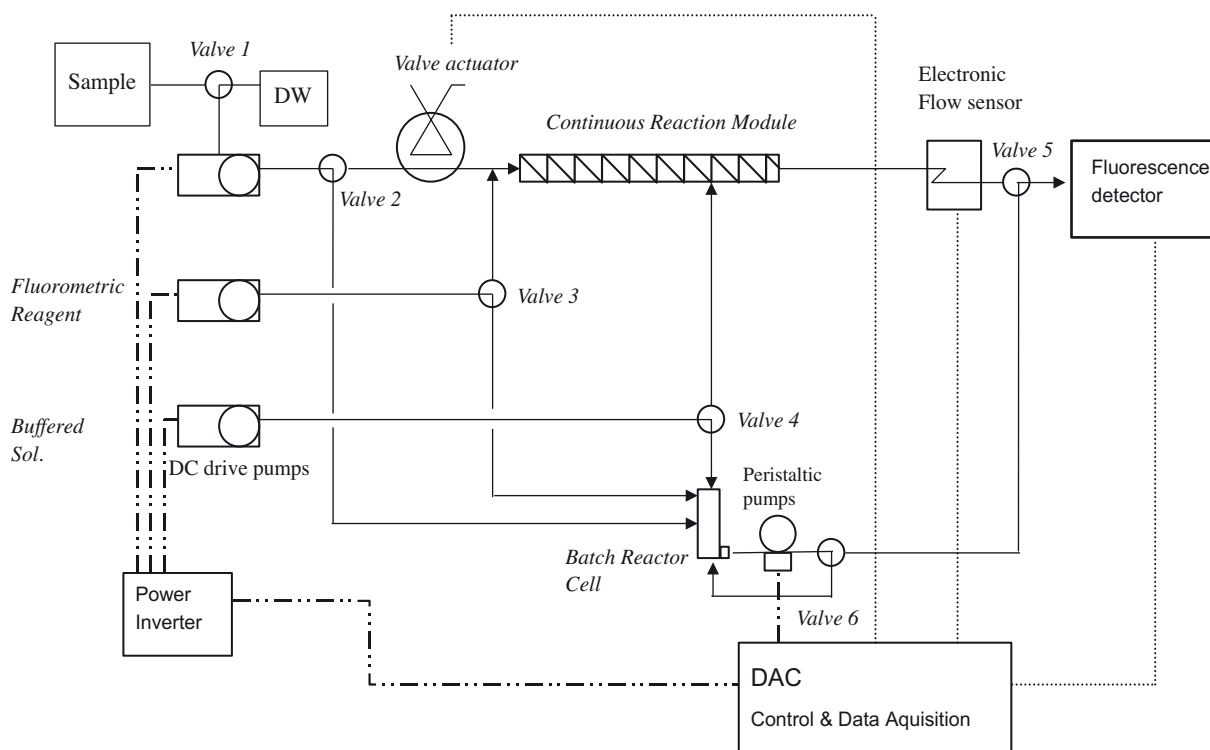


Fig. 1. Schematic diagram of the  $\text{H}_2\text{O}_2$  auto-analyzer.

continuously injected the following reagents; fluorometric reagent (0.35 M potassium hydrogen phthalate (KHP),  $8.0 \times 10^{-3}$  M *p*-hydroxyphenyl acetic acid (POPHA), 2 purpurogallin units of peroxidase/ml reagent, buffered solution (0.5 M NaOH), and the sample into the H<sub>2</sub>O<sub>2</sub> auto-analyzer, with tubing connected to the inlet and outlet of the instrument. The mixing procedure of each reagent was as follows, first, the sample was loaded into a sampling line, and if necessary, a quenching solution was added to the sample stream, using a peristaltic pump (Gilson) and three-way valve, for a few seconds. Thereafter, the fluorometric reagent enters the sample stream. When either the baseline became unsteady or significant degradation of the linearity of signal response was observed, the fluorometric reagent was discarded. Finally, buffer solution was added to the sample stream to maintain the sample above pH 10.0, as the fluorescence quantum yield of the POPHA dimer decreases below pH 9.0, but remains at a maximum above pH 10.0.

After the addition of each reagent, the reaction stream passed through either a short or a long reaction coil, according to the H<sub>2</sub>O<sub>2</sub> concentration in the sample. Solenoid valves were used for the control of mixture order of each reagent and the sample. The POPHA dimer was analyzed using a fluorescence detector (SOMA, Japan) with excitation and emission of wavelengths 320 and 400 nm, respectively. Data signals were converted into actual H<sub>2</sub>O<sub>2</sub> concentration units (μg/l) and recorded by a computer system via an interface card (Labview, USA). In this manner, the H<sub>2</sub>O<sub>2</sub> auto-analyzer could be controlled electronically.

H<sub>2</sub>O<sub>2</sub> standards were prepared by serial dilution of a stock H<sub>2</sub>O<sub>2</sub> standard, with the concentration determined by both titration with KMnO<sub>4</sub> and a H<sub>2</sub>O<sub>2</sub> assay kit (Merck). A 1% H<sub>2</sub>O<sub>2</sub> standard was prepared by dilution of commercially available 30% H<sub>2</sub>O<sub>2</sub>. The H<sub>2</sub>O<sub>2</sub> standards were freshly prepared for each experiment.

## 2.2. Tested processes

For the experiments involving UV/H<sub>2</sub>O<sub>2</sub> and ozone/UV, a 20 L reactor, equipped with four UV lamps (total UV intensity = 8 W/L and effective light path = 21 cm) and an ozone diffuser, was set up. For the experiment involving the electrochemical process, a 0.3 L reactor, equipped with a plate-type Pt/Ti electrode and a power supply (30 V), was used. In both reactors, the sample water for the H<sub>2</sub>O<sub>2</sub> measurement was able to be directly injected via a PTFE tube connected to the H<sub>2</sub>O<sub>2</sub> auto-analyzer.

## 3. Results and discussion

### 3.1. Analysis of H<sub>2</sub>O<sub>2</sub> standard solutions

Figs. 2 and 3 show the calibration curves for the H<sub>2</sub>O<sub>2</sub> standard solutions, which yielded good correlation between the H<sub>2</sub>O<sub>2</sub> concentrations and signal responses. The H<sub>2</sub>O<sub>2</sub> auto-analyzer was operated selectively using short and long reaction coils for low and high concentration ranges, respectively. From the result, the standard deviation and detection limit of 0.5 and 1.6 μg/L, respectively, were obtained from seven replicate tests (at 1 μg/L), with a coefficient of variation of 7.8%.

### 3.2. Analysis of H<sub>2</sub>O<sub>2</sub> during UV/H<sub>2</sub>O<sub>2</sub> AOP

When UV is irradiated into the water, H<sub>2</sub>O<sub>2</sub> is degraded by the reaction with photons, yielding two

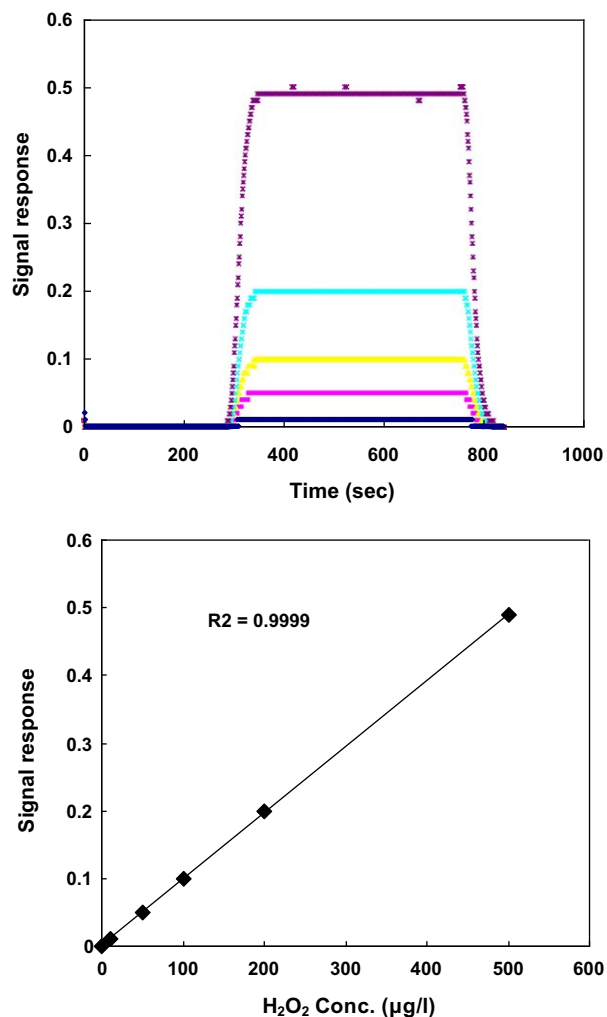


Fig. 2. Calibration curve for H<sub>2</sub>O<sub>2</sub> standard solutions at concentrations of 10, 50, 100, 200, and 500 μg/L with a short reaction coil.

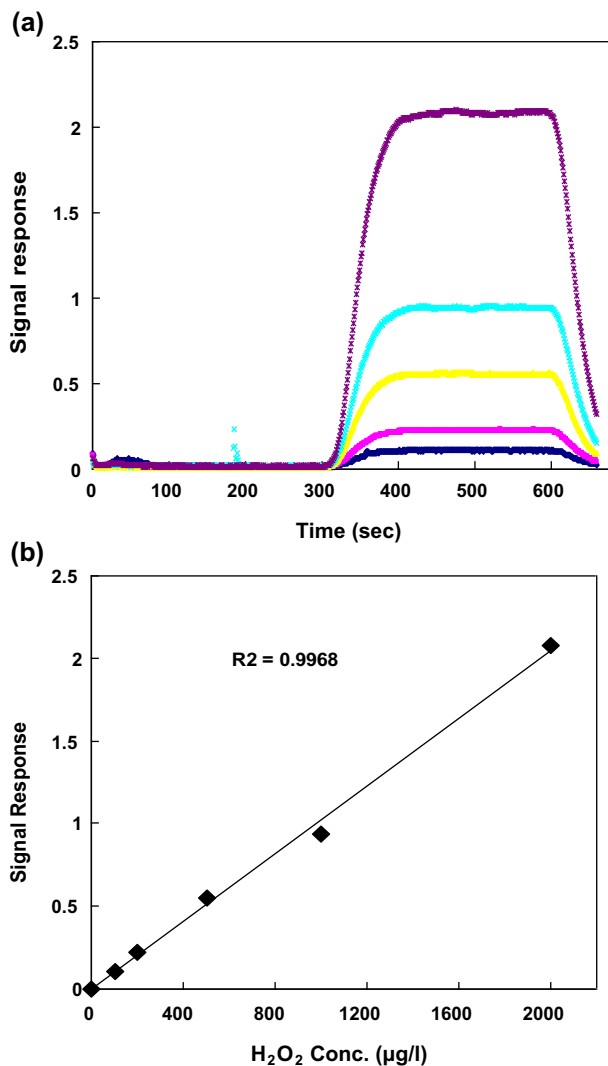


Fig. 3. Calibration curve for H<sub>2</sub>O<sub>2</sub> standard solutions at concentrations of 100, 200, 500, 1,000, and 2,000 µg/L with a long reaction coil.

moles of OH<sup>•</sup> per mole of radiation absorbed, as given by Eq. (2) [8].



The rate change of H<sub>2</sub>O<sub>2</sub> is given by the following Eq. (3):

$$-d[\text{H}_2\text{O}_2]/dt = \Phi_{\text{per,t}} I_0 f_{\text{per}} \{1 - \exp(-2.3\epsilon_{\text{per}} b [\text{H}_2\text{O}_2])\} \quad (2)$$

where  $\Phi_{\text{per,t}}$  (=about 1.0) is the overall quantum yield of the H<sub>2</sub>O<sub>2</sub> decomposition at 254 nm, as measured by Baxendale and Wilson [8],  $I_0$  is the UV intensity,  $f_{\text{per}}$  (=about 1.0) is the photolysis fraction of H<sub>2</sub>O<sub>2</sub>, and  $\epsilon_{\text{per}}$  (=17.9 M<sup>-1</sup>cm<sup>-1</sup>) the molar extinction coefficient

of hydrogen peroxide at 254 nm. In Eq. (3), if the concentration of H<sub>2</sub>O<sub>2</sub> is enough low, the term of  $\exp(-2.3\epsilon_{\text{per}} b [\text{H}_2\text{O}_2])$  can be replaced with  $\epsilon_{\text{per}} b [\text{H}_2\text{O}_2]$ , according to the Taylor series equation [9]. Therefore, Eq. (3) can be simplified and integrated as follows:

$$-d \ln[\text{H}_2\text{O}_2]/dt = \Phi_{\text{per,t}} I_0 f_{\text{per}} \epsilon_{\text{per}} b [\text{H}_2\text{O}_2] \quad (3)$$

Fig. 4 shows the removal patterns of H<sub>2</sub>O<sub>2</sub> during UV irradiation for various UV intensities ( $I_0$ ), where the H<sub>2</sub>O<sub>2</sub> decay rate increases with increasing UV intensity, as shown in the inset. This result was reasonable according to Eq. (4). From this result, the pattern of H<sub>2</sub>O<sub>2</sub> decay could be clearly observed using the H<sub>2</sub>O<sub>2</sub> auto-analyzer.

### 3.3. Analysis of H<sub>2</sub>O<sub>2</sub> during ozone/UV AOP

When measuring H<sub>2</sub>O<sub>2</sub> in the samples, the residual ozone has to be quenched as soon as the sample is injected to prevent decomposition of the H<sub>2</sub>O<sub>2</sub> from its reaction with ozone within the sampling loops. Therefore, the H<sub>2</sub>O<sub>2</sub> auto-analyzer was devised so that the residual ozone in sample could be continuously quenched, via the injection of sodium thiosulfate (Na<sub>2</sub>S<sub>2</sub>O<sub>3</sub>) using a peristaltic pump with a three-way valve connecting the Na<sub>2</sub>S<sub>2</sub>O<sub>3</sub> solution and sample lines. The quenching of the residual ozone in the sample took a few seconds, and the sample reached the fluorescence detector in 1 min. Fig. 5 shows the signal responses of H<sub>2</sub>O<sub>2</sub> at concentrations of 10, 50, 100, 200, and 500 µg/L, both with and without Na<sub>2</sub>S<sub>2</sub>O<sub>3</sub> solution. The Na<sub>2</sub>S<sub>2</sub>O<sub>3</sub> solution concentrations of 14 and 24 mM were employed, which were two times higher than theoretical concentrations able to quench 3 and 5 mg/l residual ozone, respectively. As a result, the

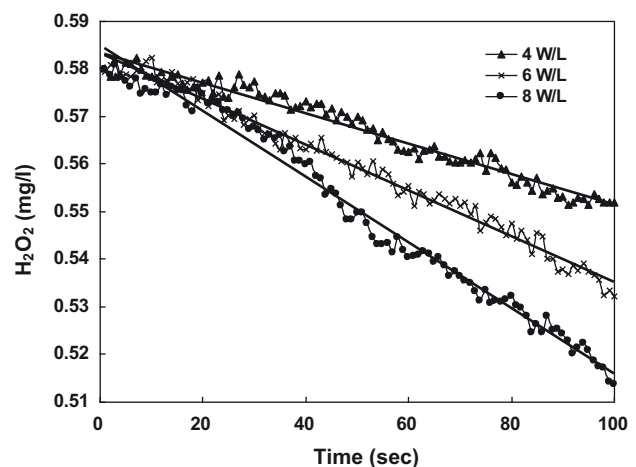


Fig. 4. Analysis of H<sub>2</sub>O<sub>2</sub> in the UV/H<sub>2</sub>O<sub>2</sub> process, [H<sub>2</sub>O<sub>2</sub>]<sub>0</sub> = 0.58 mg/L.

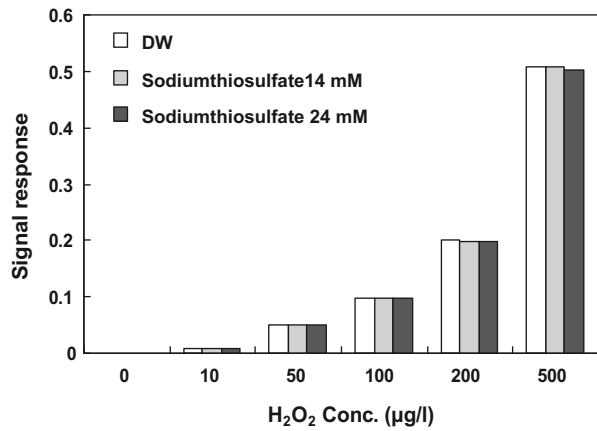
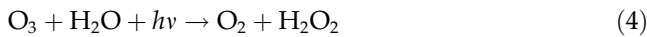


Fig. 5. Effect of sodium thiosulfate (Na<sub>2</sub>S<sub>2</sub>O<sub>3</sub>) on signal response of H<sub>2</sub>O<sub>2</sub>.

presence of Na<sub>2</sub>S<sub>2</sub>O<sub>3</sub> was confirmed to not affect the residual H<sub>2</sub>O<sub>2</sub> measurement at all.

To test the H<sub>2</sub>O<sub>2</sub> auto-analyzer, the residual H<sub>2</sub>O<sub>2</sub> was measured during the ozone/UV process, where ozone photolysis, due to UV irradiation at a wavelength of 254 nm, forms H<sub>2</sub>O<sub>2</sub> as an intermediate is the first step to obtain OH<sup>•</sup>. Taube reported that ozone photolysis in aqueous acetic acid solution led to the production of a “stoichiometric amount” of hydrogen peroxide, as shown in Eq. (5) [10]:



where the H<sub>2</sub>O<sub>2</sub> formed decays by several routes. The first is the photolysis of H<sub>2</sub>O<sub>2</sub>, which is known to yield two moles of OH<sup>•</sup> per mole of radiation absorbed,<sup>10</sup> and the second is the reaction between the conjugate base of H<sub>2</sub>O<sub>2</sub> (pK<sub>a</sub> = 11.8), HO<sub>2</sub><sup>-</sup> and ozone as, given by Eqs. (2) and (6) [11].



In Fig. 6a, the H<sub>2</sub>O<sub>2</sub> formed during the ozone/UV process was measured at various ozone dose rates. Under all ozone dose conditions, the H<sub>2</sub>O<sub>2</sub> concentration was increased with a 3 min reaction time, after which it began to decrease and then reached a steady-state level. The H<sub>2</sub>O<sub>2</sub> concentration in the ozone/UV process means that the rates of H<sub>2</sub>O<sub>2</sub> formation by ozone photolysis (Eq. (5)) and that of the decay (Eqs. (2) and (6)) were the same. It was also found that the steady-state concentration of H<sub>2</sub>O<sub>2</sub> was in proportion to the ozone dose rate, as shown in Fig. 6b. This result indicates that the H<sub>2</sub>O<sub>2</sub> auto-analyzer can be a particularly useful tool for understanding the mechanism of the ozone/UV process, and for its operation under optimum conditions.

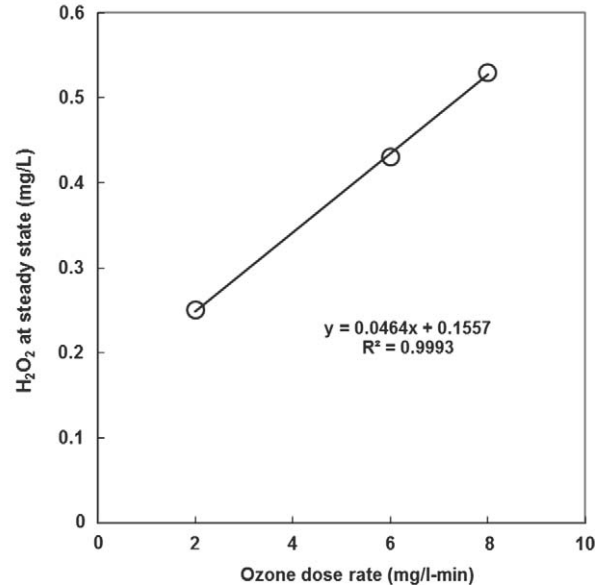
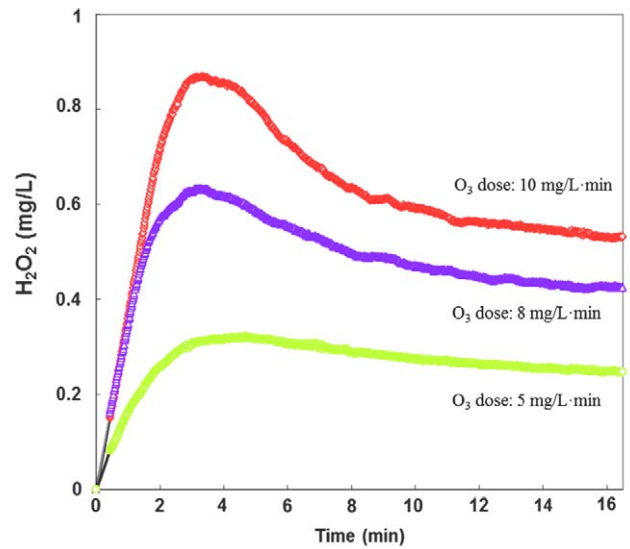


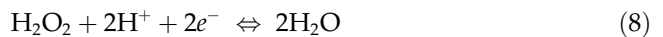
Fig. 6. Analysis of H<sub>2</sub>O<sub>2</sub> in the O<sub>3</sub>/UV process, UV intensity = 8 W/L.

### 3.4. Analysis of H<sub>2</sub>O<sub>2</sub> during electrochemical process

The H<sub>2</sub>O<sub>2</sub> formation in the electrochemical process is due to the oxidation of water that takes place at the electrode, as in the following series of equations [3]:

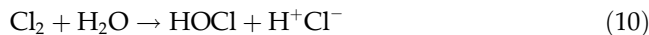


The H<sub>2</sub>O<sub>2</sub> formed can convert back to water:



This experiment was performed to detect the  $\text{H}_2\text{O}_2$  formed in pure water during the electrochemical process using a plate-type Ti/Pt electrode. The pH was controlled at 4 and 7 using  $\text{H}_2\text{SO}_4$  and  $\text{NaOH}$  solutions. Fig. 7 shows the result. Under both pH conditions, the formation of  $\text{H}_2\text{O}_2$  increased during the run time, but finally stabilized at a constant concentration. The  $\text{H}_2\text{O}_2$  formation rate was higher at pH 7 than 4. This result might be attributable to the competitive reaction between  $\text{H}_2\text{O}_2$  formation (Eq. (8)) and  $\text{H}_2\text{O}_2$  degradation (Eq. (9)). Therefore, it can be concluded that increasing the  $\text{H}^+$  concentration led to unfavorable conditions for  $\text{H}_2\text{O}_2$  formation (Eq. (8)) compared to its degradation (Eq. (9)).

When chloride ions are present in water during the electrochemical process, hypochlorous acid (HOCl) can be formed in the water, as given by Eqs. (10) and (11) [12]:



Therefore, the effect of HOCl on the measurement of  $\text{H}_2\text{O}_2$  by the  $\text{H}_2\text{O}_2$  auto-analyzer was investigated. As shown in Fig. 8, HOCl had no effect on the signal response of the  $\text{H}_2\text{O}_2$  auto-analyzer. However, when 200  $\mu\text{g}/\text{L}$   $\text{H}_2\text{O}_2$  was measured using the  $\text{H}_2\text{O}_2$  auto-analyzer, the  $\text{H}_2\text{O}_2$  concentration was immediately below half its initial level as soon as HOCl was added to the sample after approximately 4 min, and then rapidly decreased. Even though the addition of the  $\text{NH}_4\text{Cl}$  solution into the same stream, for quenching the HOCl, was performed in the same manner as that of the  $\text{Na}_2\text{S}_2\text{O}_3$  solution for the quenching of ozone, the  $\text{H}_2\text{O}_2$  concentration was only increased slightly

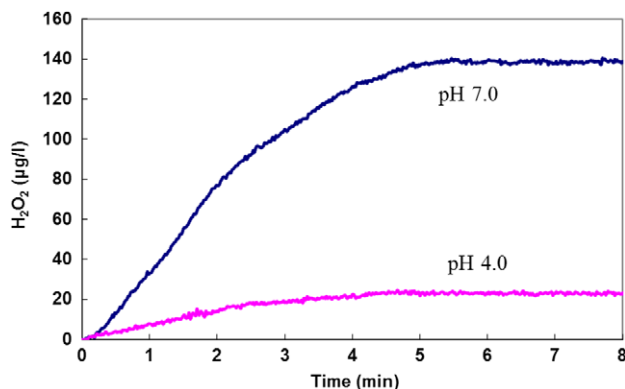


Fig. 7. Formation of  $\text{H}_2\text{O}_2$  during the electrochemical process at pH 7.0 and 4.0.

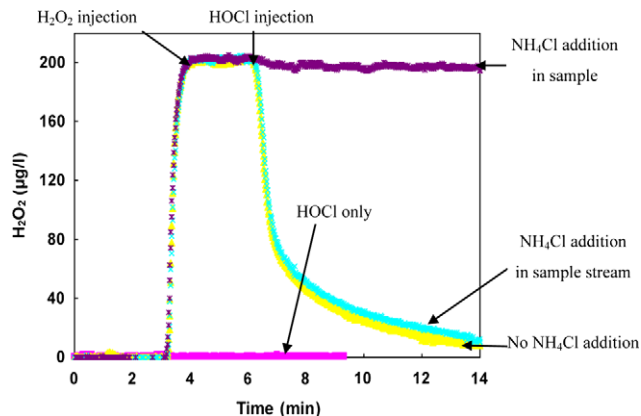


Fig. 8.  $\text{H}_2\text{O}_2$  reduction by HOCl,  $[\text{H}_2\text{O}_2]_0 = 50 \mu\text{g}/\text{L}$ ,  $[\text{HOCl}]_0 = 1 \text{mg}/\text{L}$ ,  $[\text{NH}_4\text{Cl}]_0 = 100 \text{mg}/\text{L}$ .

compared with that of no addition. This result indicates that the  $\text{H}_2\text{O}_2$  auto-analyzer can measure the pattern of  $\text{H}_2\text{O}_2$  decayed due to HOCl, but it is impossible for this instrument to measure the  $\text{H}_2\text{O}_2$  formation pattern during the electrochemical process in the presence of  $\text{Cl}^-$  leading to the formation of HOCl. In an effort to separate and detect the  $\text{H}_2\text{O}_2$ , the  $\text{NH}_4\text{Cl}$  solution was added to the sample itself. When the  $\text{NH}_4\text{Cl}$  solution was present in the sample, the  $\text{H}_2\text{O}_2$  concentration rarely decreased.

As shown in Fig. 9, to investigate the effect of  $\text{NH}_4\text{Cl}$  solution on the measurement of  $\text{H}_2\text{O}_2$ , a few samples, under various conditions, were analyzed with the  $\text{H}_2\text{O}_2$  auto-analyzer. Sample 2 ( $\text{H}_2\text{O}_2$  in  $\text{NH}_4\text{Cl}$  solution) showed almost the same signal response as Sample 1 ( $\text{H}_2\text{O}_2$  in DW), indicating that the  $\text{NH}_4\text{Cl}$  solution did not affect the  $\text{H}_2\text{O}_2$  measurement at all. Sample 4 ( $\text{H}_2\text{O}_2 + \text{HOCl}$  (1 mg/L) in

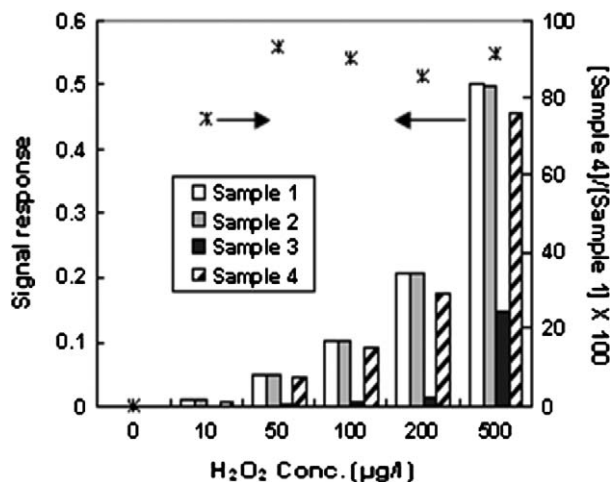


Fig. 9. Measurement of  $\text{H}_2\text{O}_2$  in the presence of HOCl and/or  $\text{NH}_4\text{Cl}$  during the electrochemical process,  $[\text{HOCl}]_0 = 5 \text{mg}/\text{L}$ ,  $[\text{NH}_4\text{Cl}]_0 = 100 \text{mg}/\text{L}$ .

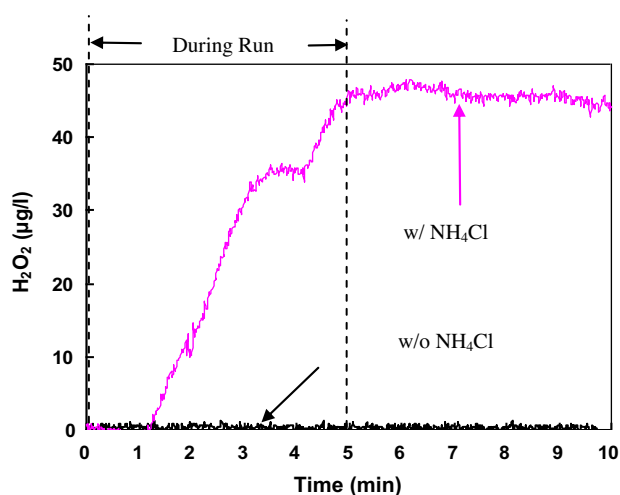


Fig. 10. Analysis of  $\text{H}_2\text{O}_2$  during the electrochemical process of tap water,  $\text{pH}=7.5$ ,  $[\text{NH}_4\text{Cl}]_0=100\text{ mg/L}$ ,  $[\text{Cl}^-]=8.5\text{ mg/L}$ .

$\text{NH}_4\text{Cl}$  solution) showed a level adjacent to that of Sample 1, overcoming the  $\text{H}_2\text{O}_2$  degradation seen in Sample 3 ( $\text{H}_2\text{O}_2+\text{HOCl}$  ( $1\text{ mg/L}$ ) in DW). The symbol (\*) represents the value calculated by (Sample 4)/(Sample 1)  $\times 100$ , with a reproducibility for Sample 4 of 85–93% within the concentration range 50–500  $\text{H}_2\text{O}_2\ \mu\text{g/L}$  (75% in 10  $\mu\text{g/L}$   $\text{H}_2\text{O}_2$ ).

Fig. 10 shows the  $\text{H}_2\text{O}_2$  concentrations present in tap water collected from Wonju city, Korea, both with and without  $\text{NH}_4\text{Cl}$  addition during the electrochemical process. For a run time of 5 min, no  $\text{H}_2\text{O}_2$  was detected in the tap water without the addition of  $\text{NH}_4\text{Cl}$ , but the formation of  $\text{H}_2\text{O}_2$  was observed with the addition of  $\text{NH}_4\text{Cl}$ . This confirmed that the  $\text{H}_2\text{O}_2$  auto-analyzer could be effectively used for measuring the  $\text{H}_2\text{O}_2$  formed in the electrochemical process.

#### 4. Conclusions

This study focused on the development and testing of an  $\text{H}_2\text{O}_2$  auto-analyzer for measuring  $\text{H}_2\text{O}_2$  using a fluorometric FIA method with peroxidase. The standard deviation and detection limit obtained were 0.5 and 1.6  $\mu\text{g/L}$ , respectively. No effects of the additions of  $\text{Na}_2\text{S}_2\text{O}_3$  and  $\text{NH}_4\text{Cl}$  to the sample stream, for the quenching of residual ozone and  $\text{HOCl}$ , respectively, were observed on the measurement of  $\text{H}_2\text{O}_2$ . To test the  $\text{H}_2\text{O}_2$  auto-analyzer, the  $\text{H}_2\text{O}_2$  removal and formation patterns in the UV/ $\text{H}_2\text{O}_2$  and ozone/UV processes, respectively, were investigated, with the

results confirming that the  $\text{H}_2\text{O}_2$  auto-analyzer could effectively measure the residual  $\text{H}_2\text{O}_2$  in each process. The analysis of  $\text{H}_2\text{O}_2$  in the electrochemical process was successfully performed, but in the presence of chloride ions, leading to the formation of  $\text{HOCl}$ , no  $\text{H}_2\text{O}_2$  formation was observed, due to the very fast reaction rate between the  $\text{H}_2\text{O}_2$  and  $\text{HOCl}$ . The addition of  $\text{NH}_4\text{Cl}$  solution into the sample made the measurement of  $\text{H}_2\text{O}_2$  possible, by inhibiting the reaction with  $\text{HOCl}$ . The reproducibility of the sample measurements, including  $\text{H}_2\text{O}_2$  and  $\text{HOCl}$  ( $1\text{ mg/L}$ ) in  $\text{NH}_4\text{Cl}$  solution, was 85–93% within the  $\text{H}_2\text{O}_2$  concentration range 50–500  $\mu\text{g/L}$ .

#### Acknowledgements

This subject is supported by the Korean Ministry of Environment as “The Eco-Innovation project (Global-Top project)” and Korea Institute of Construction Technology (KICT) as “Smart Water  $\mu$ -Grid project”.

#### References

- [1] W.H. Glaze, J.W. Kang, D.H. Chapin, The chemistry of water treatment processes involving ozone, hydrogen peroxide and ultraviolet radiation, *Ozone Sci. Eng.* 9 (1987) 335–352.
- [2] A. Chin, P.R. Bérubé, Removal of disinfection by-product precursors using ozone-UV advanced oxidation, *Water Res.* 39 (2005) 2136–2144.
- [3] R. Amadelli, A. De Battisti, D.V. Girenko, S.V. Kovalyov, A.B. Velichenko, Electrochemical oxidation of trans-3,4-dihydroxycinnamic acid at  $\text{PbO}_2$  electrodes: Direct electrolysis and ozone mediated reactions compared, *Electrochim. Acta* 46 (2000) 341–347.
- [4] G.L. Kok, Measurements of hydrogen peroxide in rainwater, *Atmos. Environ.* 14 (1980) 653–656.
- [5] K. Yoshizumi, I.N. Aokikazuyuki, O. Toshimi, K. Shujkamakura, M. Tajima, Measurements of the concentration in rainwater and the Henry’s Law constant of hydrogen peroxide, *Atmos. Environ.* 18 (1984) 395–401.
- [6] B.G. Heikes, A.L. Lazrus, G.L. Kok, S.M. Kunen, B.W. Gandrud, S.N. Gitlin, P.D. Sperry, Evidence for aqueous phase hydrogen peroxide synthesis in the troposphere, *J. Geophys. Res.* 87 (1982) 3045–3051.
- [7] G.G. Gullbault, P. Brignac, M. Juneau, New substrates for the fluorometric determination of oxidative enzymes, *Anal. Chem.* 40 (1968) 1256–1263.
- [8] J.W. Kang, K.H. Lee, A kinetic model of the hydrogen peroxide/UV process for the treatment of hazardous waste chemicals, *Environ. Eng. Sci.* 14 (1997) 183–192.
- [9] J.H. Baxendale, J.A. Wilson, The photolysis of hydrogen peroxide at high light intensities, *Trans. Faraday Soc.* 53 (1957) 344–356.
- [10] H. Taube, Photochemical reactions of ozone in solution, *Trans. Faraday Soc.* 53 (1957) 656–665.
- [11] J. Staehelin, J. Hoigne, Decomposition of ozone in water: Rate of initiation by hydroxide ions and hydrogen peroxide, *Environ. Sci. Technol.* 16 (1982) 676–681.
- [12] P. Derek, C.W. Frank, *Industrial Electrochemistry*, Blackie Academic & Professional, London, p. 269, 1993.